Collaborative Research: MRI-R2 Instrument Development of the Askaryan Radio Array, a Large-scale Radio Cherenkov Detector at the South Pole

Intellectual Merit

One of the most tantalizing questions in astronomy and astrophysics, namely the origin and the evolution of the cosmic accelerators that produce the highest energy (UHE) cosmic rays, may be best addressed through the observation of UHE cosmogenic neutrinos. Neutrinos travel from their source undeflected by magnetic fields and unimpeded by interactions with the cosmic microwave background. However, uncertainties in their predicted fluxes of make it difficult to design an array with sufficient sensitivity to collect a statistically meaningful sample of events. At high energies (above 10^{15} eV), neutrinos could be most efficiently detected in dense, radio frequency (RF) transparent media via the Askaryan effect. The abundant cold ice covering the geographic South Pole, with its exceptional RF clarity, has been host to several pioneering efforts to develop this approach, including RICE and ANITA.

Building on the expertise gained in these efforts, and the infrastructure developed in the construction of the IceCube optical Cherenkov observatory, we propose to develop an array, known as ARA (The Askaryan Radio Array), and install it in the deep ice near the geographical South Pole. South Polar ice is, in fact, perhaps the most extensively-studied on the planet; the combination of ice thickness and favorable radiofrequency dielectric characteristics, as well as the excellent scientific infrastructure and the co-location of the IceCube Observatory, makes that site unparalleled for this study. With a fiducial area of an unprecedented 80 km^2, ARA's size was chosen to ensure the detection of the flux of neutrinos "guaranteed" by the observation of the GZK cutoff by HiRes and the Pierre Auger Observatory. Within 3 years of commencing operation, the full ARA will exceed the sensitivity of any other instrument in the 0.1-10 EeV energy range by an order of magnitude. Because the antennas will be deployed in boreholes extending below the firn layer to 200 m depth, it will have the ability to distinguish surface noise from sources originating in the ice cap, otherwise not possible in the ballon borne approach employed by ANITA. Even under the extreme assumption that UHE cosmic rays are pure iron, ARA will have sufficient sensitivity to establish the presence or absence of the secondary UHE neutrinos produced by the interaction of cosmic rays with the cosmic microwave background. Such an observatory would also provide an unique probe of long baseline high energy neutrino interactions unattainable with any man-made neutrino beam.

The primary goal of the ARA array is to establish the absolute cosmogenic neutrino flux through a modest number of events. We have therefore adopted a clustered geometry in which a single localized cluster may act as a standalone array, which trades precise angular resolution for increased event rates. These events must be gold plated. The flux measurement and experience gained in operating ARA would frame the performance requirements needed to expand the array in the future to measure a larger number of neutrinos with greater angular precision in order to study their spectrum and origins.

This proposal is based on the collaborative effort of the University of Wisconsin and the University of Maryland (as sponsoring MRI institutions) with a large number of other domestic and international collaborators. The summed cumulative budget for this linked proposal is $7,931,117 over 5 years, of which $5,496,409 (69.3%) is requested from the NSF and $2,434,708 (30.7%) will be contributed by collaborating institutions in the form of cash, equipment and in-kind labor. The large-scale combination of electronics, drilling, and power/communications development, distributed among ten domestic institutions, is ideally matched to the aims of the MRI program.

Broader Impacts

Astronomy and particle astrophysics have always captured the curiosity of scientists as well as of the general public. Just as ARA will use experience from IceCube, AMANDA, RICE and ANITA to detect high energy neutrinos for astronomy and particle astrophysics studies, it will also build on the pre-existing outreach programs of those experimental efforts. Graduate, undergraduate and even high school students are already involved in studies of ARA hardware prototypes, data analysis and simulations. Our ability to immediately capitalize on established connections beyond academia affords excellent opportunities for communicating the allure of extra-galactic astrophysics, conducted in the most foreboding of terrestrial environments, to the public-at-large.

1 Instrument Location

Here we propose to develop a ~ 80 km^2 array of radio frequency (RF) antennas and install it in the Antarctic icecap near the Amundsen-Scott South Pole Station for the purpose of detecting GZK neutrinos via the Askaryan effect.

2 Research Activities to be Enabled

The detection of ultra high energy (UHE) cosmic neutrinos would yield significant science returns for both astrophysics and particle physics [1, 2]; however, uncertainties in predicted fluxes and event rates make it difficult to design an array with sufficient sensitivity to collect a statistically meaningful sample of events. One neutrino source stands out as being particularly robust - the so-called cosmogenic [3, 4] or GZK neutrinos which result from interactions of ultra high energy cosmic rays with photons from the cosmic microwave background (CMB) [5, 6]. We propose to build an array of radio receivers of ~ 80 km^2, large enough to achieve reasonable detection rates for a broad spectrum of conservative UHE cosmic ray source models and establish the flux. This detector could then form the basis for a future expanded array capable of large statistics UHE neutrino studies.

Understanding the origins of cosmic rays has been a challenge since their discovery by Hess nearly a century ago. It is now thought that most cosmic rays are ordinary nuclei accelerated to high energies in dynamic electric and magnetic fields associated with supernova explosions in our galaxy [7]; however, this explanation does not suffice for the highest energy particles, which now exceed 10^{20} eV [8, 9, 10, 11, 12]. These ultra high energy (UHE) cosmic rays must propagate to the Earth from outside our galaxy. Observations by the AUGER experiment suggest that the sources of these particles are correlated with the large scale mass distribution in the Universe [13, 14]. Although UHE cosmic rays may originate throughout the Universe, those observed at Earth must be produced near Earth because such high energy cosmic rays lose energy while propagating through the CMB ($p\gamma \rightarrow n\pi^+ \rightarrow n\mu + \nu_\mu$, etc.). This process (discussed by Greisen [5] and Zatsepin and Kuzmin [6] - GZK) not only causes energy loss for the primary, but creates secondary particles of extremely high energy [3, 4]. It is the secondary particles, particularly UHE neutrinos, which may be used to test models of the origins of cosmic rays of the highest energies [15]. With no electric charge, neutrinos do not experience scattering or energy loss, and so provide a probe of the GZK source distribution even to high redshift. Since the UHE cosmic rays have

been observed, the GZK neutrino flux models have a solid basis, although extrapolation of source models to higher redshift introduces some uncertainty. Thus, while UHE cosmic rays tell us about the recent Universe [16], UHE neutrino detection will provide crucial information at higher redshifts of z=1-4, during the epoch of structure formation.

In addition to the 'guaranteed' GZK neutrinos, it is likely that the sources of UHE cosmic rays will produce neutrinos directly [17, 18]. For example, production of UHE cosmic rays may require p-acceleration followed by a $p\gamma \rightarrow n\pi^+$ reaction and subsequent escape of the neutron, but such events also produce neutrinos [19, 20]. Cosmological relics may decay or annihilate to produce a sub-dominant UHE neutrino flux [21]. Finally, estimated event rates depend not just on the neutrino flux, but also on the neutrino-nucleon cross-section in a region inaccessible to accelerator experiments. The proposed detector is sized assuming calculated Standard Model cross-sections [22]. With sufficient statistics, these predictions can be tested by determining the differential event rate near the horizon [23, 24]. An extreme possibility would be to discover significantly enhanced cross-sections, such as occur in fundamental theories with extra dimensions. We view these challenges as opportunities.

The detection of UHE GZK neutrinos is an experimental challenge at the frontier of neutrino astronomy, which has progressed over the last half century from initial detections of low energy thermal neutrinos from our sun [25, 26], to detection of modest energy neutrinos produced by cosmic ray interactions in Earth's atmosphere [27], to the current efforts of the IceCube [28, 29] and Antares [30] collaborations to detect higher energy neutrinos from sources outside our solar system. With each increase in neutrino energy, the required detector increases in size as the flux decreases dramatically with energy. At 1 km^3, the IceCube Observatory is still too small to detect GZK neutrinos with a reasonable rate, and the technology is too costly to scale up to the ~ 80 km^2 envisioned here.

With the primary goal of discovering the GZK neutrino and establishing its spectrum, the proposed radio receiver array is necessarily sparse. We maintain energy sensitivity down to $E \simeq 10^{17}$ eV by adopting a cluster ("station") design. We estimate an angular resolution for the reconstructed direction of the incoming neutrino at $\sim 10°$. At high redshift ($z > 1$), GZK neutrinos are produced within 6 Mpc ($< 5'$), of the associated UHE cosmic ray source. Our proposed instrument is not likely to perform classical neutrino astronomy, but the reso-

Table 1: Collaboration personnel who will participate in array development and data analysis.

Institution	Funding	Personnel Category[†]			
		[1]	[2]	[3]	[4]
US Participants:					
Univ. Wisconsin	NSF	2	1	1	2
Univ. Maryland	NSF	2	1	2	2
Univ. Hawaii		2	2		
Univ. Kansas	NSF	1		2	12
Univ. Delaware	NSF	1	1	1	1
Ohio State Univ.	NSF	1	1		
Univ. Alabama	NSF	1			1
Colorado St. Univ.	NSF	1		1	2
Penn St Univ.	NSF	1		1	
Univ. Nebraska	NSF	1			1
Taiwan:					
Nat'l Taiwan Univ.	LeCosPA NSC	1	2	7	1
Belgium:					
Univ. Bruxelles	FNRS	2	1	1	1
United Kingdom:					
Univ. Coll. London		2	1	2	2
Japan:					
Chiba Univ.	JSPS	1	1	1	1
Germany:					
DESY	BMBF	1		1	
Univ. Wuppertal	BMBF	1		1	

[†][1] Senior Personnel;[2] Postdocs;[3] Grad. Students;
[4] Undergrads.

lution is sufficient to enable measurement of neutrino nucleon cross-sections, and the sky distribution of events will verify basic operation of the detector and identify the source events as cosmic neutrinos.

The construction of the proposed array will be a technological challenge, however, there is great interest within the particle astrophysics community in the scientific window that such a frontier instrument is sure to open and a large international collaboration has already formed, with many foreign universities bringing significant resources to the project. A list of participating institutions, with the number of scientists collaborating at each, is shown in Table 1. These numbers are expected to grow as the array begins collecting data. The participants are comprised of scientists from the IceCube and AMANDA polar optical Cherenkov observatories, the RICE and ANITA radio Askaryan telescopes, as well as the Pierre Auger cosmic ray observatory, who together form a broad base of technical and scientific expertise that will be invaluable to the success of the project. The results of the most relevant prior NSF funding awarded to this proposal's PI's are summarized below.

2.1 Results from prior funding

IceCube [28], which is currently under construction at the South Pole, will be the world's largest neutrino observatory (in instrumented volume) and will provide a new window on the universe at TeV (10^{12} eV)- PeV (10^{15} eV) energies, where cosmic ray protons provide no directional information. IceCube was funded through an MRE from the NSF that was administered by the University of Wisconsin including PI Albrecht Karle, with several other ARA members participating. The construction of such a massive array in the harsh polar environment was ambitious, but the installation is on schedule, with 59 of the planned 86 strings of phototubes already installed and sending data north for analysis. During the past calendar year, the array has been operated with nearly 95% live time, even during construction activities. A number of IceCube results have already been published, including a search for point sources of neutrinos with the first 22 strings of IceCube [31], an indirect search for neutralino annihilations in the Sun [32], and a dedicated search for neutrinos in coincidence with a bright GRB observed by optical observatories March of 2008 [33].

Also located at the South Pole, the RICE experiment pioneered the technique, employed by ARA, of using an englacial array of antennas to search for UHE neutrino interactions via their characteristic impulsive radio emissions. It has been accumulating data continuously over the last ten years, save for an eight-month interruption in 2008. The most recent science result has been a search for ultra-relativistic magnetic monopoles in the RICE data [34]. A complete re-analysis of the existing RICE data set is underway and should result in an enhanced neutrino detection sensitivity of approximately 50% relative to the most recently published RICE results.

Under the auspices of a recent OPP grant (NARC, for "Neutrino Array Radio Calibration"), the science mission of RICE was extended to include necessary calibration groundwork prior to the initiation of ARA. That work has included: i) the measurement of an upper limit on the (vertically-integrated) birefringent-asymmetry of South Polar ice at <0.01%, in contrast to non-zero measurements made at Dome Fuji, and Taylor Dome[35, 36], and ii) the addition of surface antenna channels to the pre-existing RICE DAQ in an attempt to measure the geosynchrotron radio emissions expected to accompany the Extensive Air Showers measured by the IceTop experiment. Correspondingly, the RICE trigger has been re-configured to admit such air shower triggers during 2009 data-taking.

Within the context of NARC, five digital radio module (DRM [37, 38]) clusters were co-deployed with IceCube in the austral summers of 2006-07 and 2008-09 to depths of $\sim 250 - 1500$ m. These clusters are a joint effort of a RICE-ANITA-IceCube
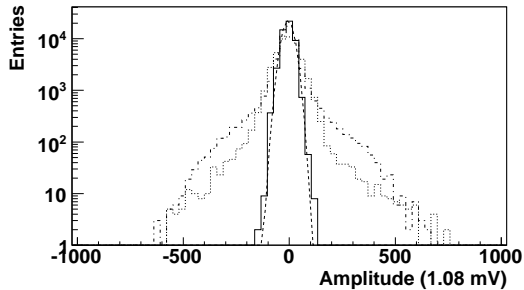
Figure 1: Signal Voltage distribution for a single channel (single antenna) for ambient thermal background (dashed line) with a fit to a Gaussian (solid). Also shown is the voltage distribution for triggered events in two threshold settings (dotted lines).

team and uses the RICE concept of deep ice detection of neutrinos, with ANITA based fast digitizer electronics, combined with IceCube deep ice holes, communications, and power infrastructure. There are many similarities with the proposed ARA: Each cluster consists of 4 receiver antennas equally spaced, the triggering is based on frequency banding and coincidence hits from several antennas within a cluster, and the digitization is performed using the 260-capacitors Switched Capacitor Array LABRADOR [39] chip sampling at 2 GSPS with 512 bins depth. The concept of detecting short pulses by fast sampling and digitization near the receiving antennas in the deep ice environment has proven successful, and ARA will use similar (improved) electronics. Using hits information from a single cluster, we have made routine zenith angle calculations and thereby discriminated up-going from down-going events, as proposed for ARA. The cluster geometry described herein allows 3-D reconstruction of the vertex point, with considerably better resolution. Our NARC in-ice deployments have also demonstrated that the in-ice environment (including all nearby electronics) is consistent with the expected black-body Gaussian thermal noise environment.

Figure 1 shows the voltage distribution for one channel on one of the clusters. The ambient background nicely fits a Gaussian with RMS of up to 30 mV (with variations between channels). Further studies are being done with the recently deployed clusters, including in-ice transient and ambient deep ice backgrounds, RF attenuation length, biweekly RICE transmitter reconstruction calibration, and coincidences with both RICE and the IceTop array.

3 Research Instrumentation and Needs

The proposal to detect coherent radiation from particle cascades is due to Askaryan [40]. An EeV neutrino which interacts in the ice produces a forward moving cascade of secondary particles. The cascade carries a net negative charge, balancing the positive charge of the ionized nuclei left behind. In essence, the charged cascade is a spark of length 5 m and radial size 10 cm. The radiation pattern from this spark is determined by the spatial and temporal current distributions. In this case, the particles form a relativistic pancake, and so the emission resembles Cerenkov radiation, propagating outward from the cascade in a conical wavefront of 5 degrees halfwidth and a temporal thickness of a few nanoseconds. The basic nature of the Askaryan process has been demonstrated in a series of experiments at SLAC [41, 42, 43]. The details of the radiation pattern have been calculated consistently by several groups, most notably Alvarez-Muniz and Zas and collaborators [44], and these calculations of radiated power and its energy dependence agree well with the measured values.

3.1 Instrument Overview

We propose to construct a radio-based neutrino detector array covering a physical area of $\sim$ 80 km^2 (Figure 2) at the South Pole (SP). The full ARA will be a discovery-class instrument designed to detect of order 5-10 UHE neutrino events per year based on current models, and would serve as the core for expanding to larger precision measurement observatory class arrays of 300 to 1000 km^2, capable of detecting hundreds of GZK neutrinos per year. The location near the SP station has the added advantage of providing co-location with IceCube. A small but extremely important fraction of all UHE neutrino events detected will produce a signal in IceCube as well, and this synergy in detection will benefit the scientific goals of both instruments. In this context, we note that at some of our collaborating German institutions, ongoing R&D programs are investigating the enhanced GZK neutrino detection potential offered by the complementary acoustic [45, 46] technique.

An overview of the layout of the instrument relative to the SP station is shown in Figure 2.

3.2 Rationale for Proposed Instrumentation

There is a heirarchy of important science motivations for UHE neutrino detection. At the foundation level, the absolute flux level of the cosmogenic neutrinos sets immediate constraints on the parent distribution of the highest energy cosmic ray sources at all cosmic epochs. This goal requires a small set of well-established events, and informs the design of all subsequent detector expansions. Second, measurements of the energy spectral content of the neutrinos determines characteristics of the cosmic evolution of the parent source luminosity. This goal requires many dozens of events so that there is enough statistical power to begin to delineate the
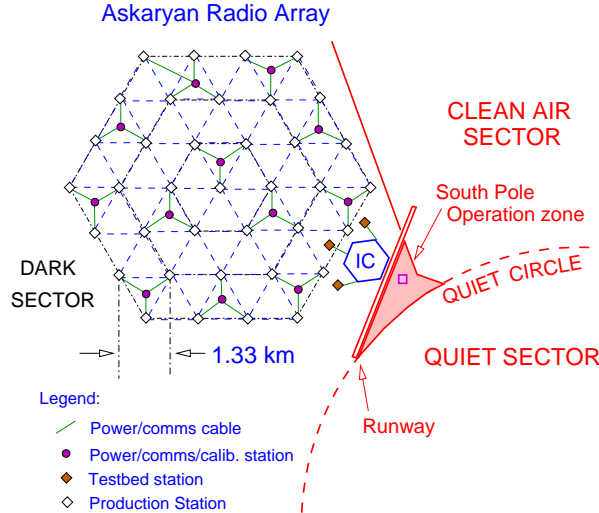
Figure 2: Planned layout of the 37 ARA stations with respect to the South Pole Station and associated sectors.
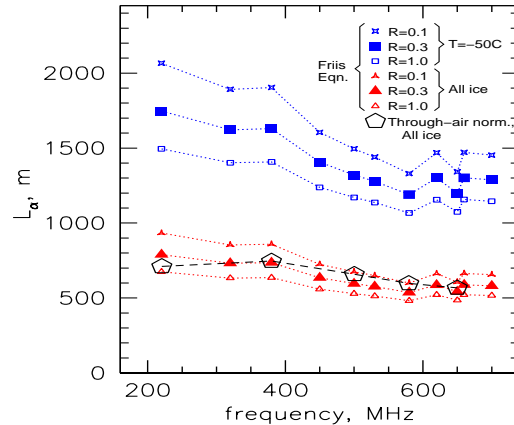

Figure 3: Ice Attenuation measurements made at the South Pole in 2004 [47], indicating the extremely long attenuation lengths that obtain down to depths of 2 km for which the average temperature is -46C [48].

spectral energy distribution of the neutrinos. Third, high angular resolution studies of possible sources can begin to unravel the details of their association with visible matter in the universe. This goal requires both a larger statistical sample of events, and high angular resolution on the neutrino direction, initially at the 0.1 rad scale, but eventually at the arcminute level. Finally, once the neutrino fluxes are established, and events can be characterized with some precision, studies involving the flavor and neutral vs. charged current distribution of the neutrinos can begin. This final goal, in which a rich harvest of fundamental physics results is possible, builds upon the previous elements in the heirarchy, and will require very large, fine-grained detectors collecting high statistics, certainly in the hundreds of events per year at least.

The current instrument will address the primary foundation of this heirarchy of physics and astrophysics goals by establishing the absolute flux level. It can also begin to address the goal of determining source directions on a subset of events, as well as first order energy spectral parameters. However, our primary rationale for the proposed design is weighted most strongly toward robust detection and measurement of the absolute flux. This motivation leads us toward a design in which the elements of the detector array are individually able to identify neutrino events without requiring that multiple widely-spaced elements receive coincident hits. The solid-angle – of order 0.5 sr – into which the radio Cherenkov cone is emitted is relatively small and limits the number of multiply-illuminated stations in a coarsely-gridded array, thus favoring our approach where each of the 37 instrument stations can independently trigger and reconstruct neutrino events. The spacing of the array elements, in this case the individual stations which support the underice antenna clusters, is dictated by the attenuation length of the ice, which in turn is largely determined by its temperature. Ice at the South Pole is extremely cold, averaging -46C over the range from the surface down to 2 km depth [48]. This in turn leads to a field attenuation length well over 1 km in the frequency range of interest, as shown in direct measurements (Figure 3).

To design a single, relatively small cluster of antennas capable of identifying a neutrino interaction, we have relied heavily on the proven design of the Antarctic Impulsive Transient Antenna (ANITA) long-duration balloon payload, which synoptically views the Antarctic ice sheet from 36 km balloon altitudes, and precisely locates event directions using a small cluster of well-characterized antennas arrayed to form a pulse-phase radio interferometer. As we will show below, ANITA has demonstrated the potential power of the cluster detector approach. However, by deploying in-ice, ARA has the ability to discriminate surface from sub-surface sources not otherwise possible with the synoptic approach. This was the approach pioneered by RICE, which has demonstrated the feasibility of an embedded array. The vertical dipole antennas developed for RICE are ideal for installation in narrow boreholes and have excellent response. Finally, Ice-Cube brings considerable experience in ice drilling and logistics in the harsh polar environment. We have adopted several of the features of the ANITA, RICE and IceCube methodologies in designing our instrument.
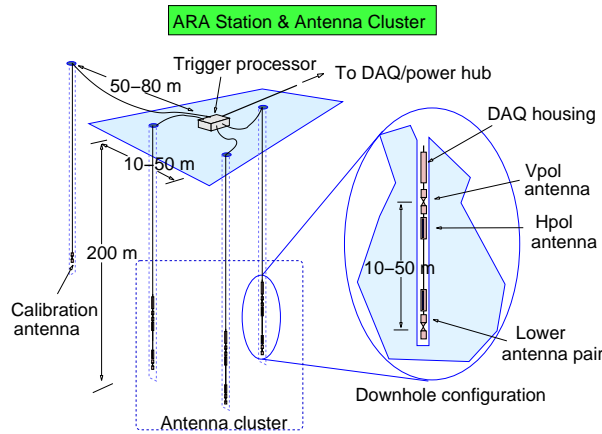
4

Figure 4: ARA Station layout and antenna cluster geometry.

3.3 Design Concept

3.3.1 Array & cluster geometry

The individual stations consist of a triad of boreholes with diameter of 10-15 cm, and depths of 200 m, on the corners of an equilateral triangle with sides in the range of 10-50 m, with spacing to be optimized during the design phase of the project. Figure 4 gives a schematic view of the layout. Within each borehole are two pairs of horizontally (Hpol) and vertically polarized (Vpol) antennas. The antenna Hpol+Vpol pairs are vertically separated by spacings comparable to the borehole spacing.

The 12 antennas of a cluster station are serviced by a single trigger processor and controller module located at the surface above the boreholes. This module communicates via a 600 m cable to a nearby data acquisition, communication, and power hub located so as to serve three nearby cluster stations. Communication with the central data center is done via this hub, and power for the cluster is received from it. As described above, the clusters then lie on a hexagonal lattice with 37 stations. A central location is provided for the DAQ center, and the 12 required power/communication hubs are located at the interstices of the hexagonal grid. A total of just over 7 km of trenched cable services the array from the power/communication hubs.

3.3.2 Antennas & Receivers

The antennas used for the clusters are of two types: the Vpol antennas are wideband dipoles developed for the Radio Cherenkov Ice Experiment (RICE), and will be operated over a passband of 200-650 MHz, over which their performance has been verified to be excellent. For Hpol operation, slotted cylinder antennas are the electromagnetic complement of vertically polarized dipoles, and have been studied for many years for operation in the confined geometry of boreholes. We plan to use a

design that will be optimized for matching with the RICE dipoles. Both Hpol and Vpol antennas retain a $\cos^2 \theta$ dependence of their power response as a function of zenith angle θ, offering complete polar angle coverage for neutrino detection.

Each antenna will have an associated low-noise amplifier (LNA) module coupled to it as closely as possible and powered via a bias tee along its receiving coaxial cable. This minimizes the additive noise due to any cable loss, which is magnified by the fact that any attenuation prior to the first LNA stage causes both signal loss, and increases the noise figure of the system, a double hit in sensitivity. The LNA module includes a passband filter as its first component, prior to the LNA itself, to ensure that no out-of-band interference source can cause degradation of the noise performance of the system. At the LNA input we also include an integrated RF power limiter, which provides protection against strong RF transients that might occur at any time during the fabrication, deployment, or operation of the system.

For this LNA module we follow the basic approach verified in the ANITA-2 flight system, which demonstrated a system noise temperature of under 90 K at room temperature. For the ambient temperature expected in ARA, we estimate that this should improve by 20% to 70 K or better – an outstanding performance level for a non-cryogenic broadband amplifier. Following this 38 dB gain LNA module, a second-stage amplifier (SSA) is used to boost the signals by another 38 dB. This brings thermal noise to rms voltage levels of order 100 mV in a 50Ω receiving system, fully adequate for the follow-on electronics.

3.3.3 Trigger & Digitizers

The array electronics consist of three distinct hierarchical components, as shown schematically in Figure 5. A station comprises 3 strings, each servicing 4 antennas; the combined 12 antennas form a *cluster*. The outputs from the antenna SSAs are split by an RF coupler; a portion of the signal is used for waveform sampling, and the remaining portion is fed into a Analog Device AD8318 logarithmic amplier / power detector (log amp), which produces a voltage of the instantaneous signal power but retains response times of order nanoseconds. The log amp signals are used to make real-time trigger decisions and monitor the ambient RF power. The concept of developing a detection system based solely on the information content of the log amp has been and continues to be explored by several members in the collaboration. We plan to deploy several sensor strings equipped with this simplified readout

configuration in order to ascertain the performance of these detectors both as the triggering system for the waveform capture hardware and as a potential stand-alone technology. These sensors would be deployed inside one of the first super-clusters and allow redundant data for additional tests on systematic effects and calibration.

Each LA output is fanned-out into 5 trigger inputs and an analog multiplexer (the latter not shown). The analog multiplexer steps through all 4 antenna channels and feeds the output to a slow ADC (also not shown), which provides periodic updates of the RF power for monitoring as part of the system health (housekeeping) portion of the data stream. Several copies of the LA output are sent into one polarity of differential receiver inputs on the FPGA. The other polarity input of the differential pair is driven from a multi-channel Digital-to-Analog Converter (DAC) to set the threshold. Using internal firmware to form an updating 1-shot circuit, each of these LA channels then function as discriminators[49, 50], which are used to provide both triggering and TD measurements.

At the primary output of the RF couplers, the signals are fed into the Ice Radio Sampler (IRS) Application Specific Integrated Circuit (ASIC). This Switched Capacitor Array device is based upon experience with a very similar ASIC (LABRADOR) [39] flown successfully twice on the ANITA payload and subsequently used in a number of physics applications, as well as the AURA array. A major difference of the IRS ASIC is the much larger analog buffer depth, however the principle is the same. Low power operation is realized by converting the analog samples to digital values only when triggered, which happens at the 1-100Hz rate. Upon receipt of a trigger, samples in the trigger window are digitized and then either collected for event building, or stored into a local buffer, as described below. We plan to digitize at 2 Gsamples/sec, which is matched to the IRS specification. Each analog sample is digitized to 12 bits of resolution, though 10 effective bits are expected (1mV noise floor and 1V dynamic range). Conversion and readout latency is expected to require about 100 microseconds. During this interval, no deadtime is incurred since sampling will continue using storage cells that are not part of the window of interest.

As depicted in the lower part of the Trigger/Control FPGA in Figure 5, the FPGA firmware allows a wide flexibility in configuring the exact states required for a trigger. The general trigger conditions always involve some coincident combination of impulses from a subset of antennas in the cluster within a time window large enough (of order 100 ns for 10 m intracluster spacing) to accommodate a wide set of arrival directions. These triggers can originate either from an actual incident EM wave of external origin, or may be due to a fluctuation in thermal noise power. The latter events can be either locally rejected prior to saving of the waveform, if they do not satisfy causality required for a coherent EM wave, or they may be saved for offline analysis if the rate of such accidentals does not pose a problem for the instrument data bandwidth. Such *thermal noise* triggers are useful for establishing instrument health and for absolute sensitivity calculations. As we have learned in the ANITA and RICE experiments, even when such accidental triggers satisfy first-order causality conditions they are easily rejected at high confidence once the waveform phase and Fourier spectral information are analyzed, and they pose no background to real neutrino events. We have done a comprehensive initial study of trigger conditions for the 12-antenna cluster in our current baseline design, and we find that there are a range of conditions which yield good sensitivity; we have adopted a simple 5-out-of-12 coincidence for our current analysis.

The trigger threshold also allows for several levels, and firmware control can then provide several types of response sequence. For example, conditions may be set where the TD signals can all be broadcast over a small amount of the available link bandwidth to the Central Station, and because no waveforms are stored a long record of these lower-level triggers can be logged into a deep RAM buffer, providing up to 10 s of storage for low-level transients at a sub-trigger threshold. This permits us to investigate coincident IceCube triggers and to broadcast these for capture to the Cluster Controller from the Central Station. The Cluster Controller forwards the requested time window to each of the String Controllers, whose State Machines then queue hits in the Deep RAM buffers corresponding to the requested time window. All of these queued events–TD and waveform data–are streamed back to the Central Station for processing. As with threshold settings, all trigger settings can be tuned or updated from the Central Station (remotely). A GPS receiver is planned for each Cluster Controller in order to time stamp events. This mechanism will be augmented with a separate common timing marker, broadcast from the Central Station, to overcome limitations on the available timing possible with the GPS receivers at the sub-10ns level.

At the Central Station, the array Data Acquisition (DAQ) and trigger are shown schematically.
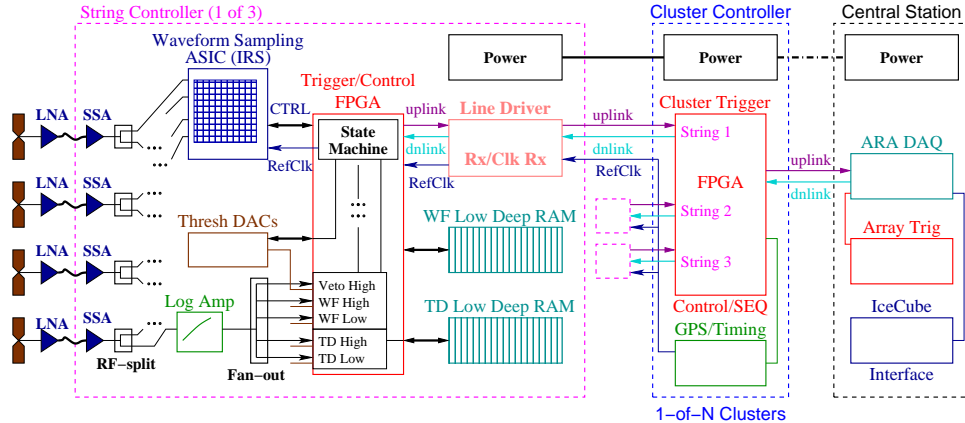
Figure 5: Schematic of the ARA instrument & data flow. Greater detail is shown for the systems most critical to instrument functionality.

We baseline a 1Mbit/s link uplink rate (downlink can be lower bandwidth). An event (with 10% overhead for housekeeping and timestamp data) is about 26kbits (3.3kBytes), corresponding to a baseline cluster trigger rate of about 6 Hz, or about 220 Hz for the full ARA. Another 10% of the bandwidth can be devoted to TD data. This 16kbit/s pipe permits a rate of a few hundred Hz per station of these events, depending upon the timing resolution and roll-over period allowed on the timestamp. The remaining bandwidth is available for array trigger requests and link margin. This yields a raw data accumulation rate of 300 Gbyte/day, which is decimated at the central DAQ station via a small set of data servers, down to a subset of about 20 Gbyte/day which can be transfered via satellite communication to the ARA Consortium university data centers.

3.3.4 Control, Communications, & Power

During initial phases of the instrument development, ARA will employ trenched cables to deliver power and communications to the first prototype stations that are deployed. This will allow flexibility during this development period, but it is not a sustainable solution for a very large array covering 80 km^2. For the larger array we will begin early on to develop the Power/Comms Hub (PCH) architecture outlined above. In this scheme, power is provided by a combined wind turbine/solar photovoltaic (PV) station centered at the interstices of the hexagonal grid as shown in Figure 2.

The high Antarctic plateau has particular challenges for wind power: lower wind speed than the coastal regions (with occasional outages), and very low temperature. Initial efforts in the 1990's were hampered by reduced bearing lubricant viscosity with decreasing temperature, resulting in bearings that locked below -60C during wind outages. More

recent implementations (within the last five years) have demonstrated year-round performance, interrupted only by periods when local wind speed falls below threshold (4 m/s) for more than 48 hours. These outages are much more likely during the austral summer, when PVs have been proven effective.

Recent successful Antarctic efforts have included a Major Research Instrumentation grant awarded to UNAVCO/IRIS (2006 to present) [51], the Automated Geophysical Observatory (AGO) deployments (2004-present) [52] and the Autonomous Real-time Remote Observatory (ARRO) project [53], as well as R&D work to power South Pole Station itself via wind turbines. The UNAVCO and AGO turbines are inspected yearly and, if needed, lubricant and bearings replaced.

Each ARA super-cluster will be powered by one or more wind turbines of a type that has been in use already in Antarctica for the last 2-5 years. The AWP turbine, successfully used in AGO installations, delivers roughly twice the power needs for each station, while the UNAVCO model is too small by a factor of three. In our discussions with UNAVCO, they have offered either a larger-scale version of their already deployed units, or smaller turbines operated in parallel. The key factors under consideration are cut-in wind speed, proven bearings, proven lubricant, cold-resistant construction materials, and tolerable RFI. The AWP is a proven backup which can be used if the scaled-up UNAVCO version proves inadequate.

To survive the wind outages, UNAVCO employs a gel Sealed Lead-Acid (SLA) battery bank installed in an insulated enclosure. We currently favor PVs as a more cost-effective solution. Careful attention to the charger controller will be required to handle not only charging from two or more sources but

successful recovery in the case of a cold soak.

At each interstitial ("supercluster") location, a low-power wireless communication module will be installed, based on ruggedized 925 MHz systems (above our band of interest) in use in Alaska. The required bandwidth for the wireless communication is ≈1-2Mbps for the expected operational data throughput from each station. Each of the remote stations would communicate data to the central communications receiver at the IceCube Laboratory. The IceCube project has identified adequate space for the two racks of electronics required. (More space could be made available if needed.) The reduced data output of 20 GB/day will be then incorporated into the daily South Pole data stream (via satellite) for storage at UW or UMD, where data will then be made accessible to the collaboration.

3.3.5 *In Situ* Calibration

In addition to the single local calibration antennas nearby the clusters, we will provide a longer range underice calibration pulser capable of being detected by multiple clusters. Coincident with the PCH we will co-locate a single borehole, also 200 m deep, in which a calibration antenna will be placed along with an impulse generator which can be activated and triggered from the surface PCH station. These calibration modules will be visible to three adjacent clusters and will provide realtime monitoring of the vertex reconstruction capability of each cluster, as well as amplitude and other timing information. In addition, these signals will provide both near-term characterization and long-term monitoring of ice properties in the ice target region.

Two other calibration methodologies are planned for operation. The first will be done shortly after the deployment of each cluster, and whenever necessary thereafter. This calibration involves use of surface antennas and signal sources broadcast into the cluster at ranges of 50-100 m on the surface. It will enable a complete azimuthal scan of the cluster response function for a given set of elevation angles, and will help provide ground-truth information to detailed antenna modeling code which will then provide analytic continuation of the antenna parameters in regions where they are not well-sampled.

Clusters can also be calibrated on solar radio fluxes by using correlation interferometry among the cluster antennas. This type of interferometry is directly analogous to radio astronomical imaging, and has been employed successfully by the ANITA experiment to perform radiometric and timing calibration of the ANITA antennas during flight. The Sun is a very strong radio source at 200-650 MHz, but because of its small angular extent (nearly the
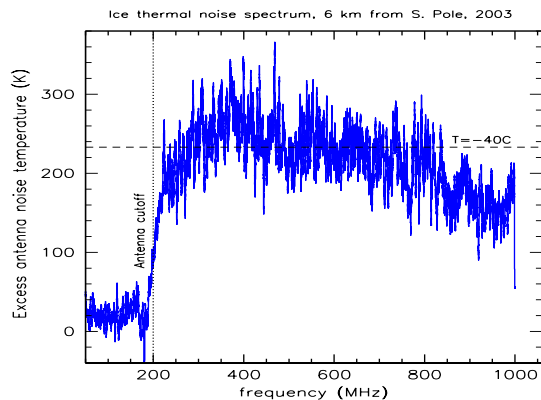

Figure 6: Thermal noise measurements of ice at 6 km from SP station in 2003. No strong EMI was observed in the spectral region of interest for ARA at this time.

same as the visible Sun) it does not contribute much to the overall thermal noise background, since the low-directionality antennas integrate over their entire surrounding solid angle. However, when the antennas are correlated interferometrically, they can resolve the correlated radio noise from the direction of the solar disk, allowing a first-order gain calibration tied directly to known solar flux densities.

Finally, we note that air showers cores reaching into the ice may provide a test beam for this cluster [54]. These investigations are still at an early stage and are not part of this funding proposal but will be part of ancillary funding requests in Europe.

3.3.6 Interference

Electromagnetic interference in the vicinity of the SP station is a valid concern, and we have done extensive evaluation of these issues in developing our instrument development plan. We have made measurements of the impulsive RF noise environment at distances from SP station comparable to the center of our planned array, as shown in Figure 6. Measurements made with the RICE/NARC arrays (cf. Figure 1 above) also established the close-in EMI levels, and strategies to mitigate them in triggering and via hardware notch filtering, where necessary, have been routinely achieving 10^3 : 1 online background rejection factors for several years.

3.4 Development Strategy

In our initial year we will deploy two surface stations that are being developed through in-house funding from Hawaii, Wisconsin, and Taiwan. These stations will be deployed with a DAQ that interfaces already to IceCube DAQ infrastructure. These stations are prototypes of our current ARA station, except that they only support near-surface antennas, down to several m at most. They will serve to establish any issues with EMI that need to be addressed in the ARA design, and will help determine cluster trigger parameters with *in*

8

situ operation, as well as delineating the deployment and commissioning sequence needed for the larger-scale station deployments. Design and engineering model development of the baseline ARA stations will continue at the design level in the first year and into the 2nd year, during which between 3-5 phase-I stations will be constructed and then deployed. Design reviews and production readiness reviews will be scheduled to avoid or minimize design changes. The third through the fifth year will be focused on production and the deployment of the remaining stations.

3.5 Construction and Deployment

The sensor strings will be deployed into boreholes of 200 m depth and 10 to 15 cm diameter. We have selected the so-called Rapid Air Movement (RAM) drill as the baseline drill, following a series of workshops and meetings by experts in RAM and hot water drilling technologies. The RAM drill has been used routinely at WAIS Divide for 50 m deep holes; drilling to 200 m should require approximately 2–4 hours per hole with an upgraded drill. The plan foresees commissioning of the drill at the South Pole in the second deployment season. We estimate that combined drilling and deployment operations will require about 6 people during an 8 week season. Details of the moderate support requirements are documented in the ORW (Operations requirements worksheet), which also includes requirements for the sensor deployment, cabling and wind turbine installations.

3.6 Expected Performance

We characterize the expected performance of ARA based on an extensive suite of Monte Carlo and other simulation and modeling tools developed over the last two decades. Several of the investigators on this proposal have been involved in radio methods for detection of UHE neutrinos since the mid-1990's and thus the heritage of our simulation methodology is many generations deep and has been proven over a wide range of active and completed experiments, including the RICE [55] and IceCube radio [37, 38] experiments, which are direct pre-cursors to ARA, the Goldstone Lunar Ultra-high energy neutrino Experiment (GLUE) [56], and the ANITA experiment [57].

Our Monte Carlo tools include detailed ice attenuation modeling and raytracing to account for the gradient in the index of refraction of the ice vs. depth. They provide state-of-the-art modeling of the Askaryan radiation from showers via tested parameterizations, which have been validated by direct measurements of the Askaryan effect in ice at SLAC [43]. Neutrino propagation through the earth

and ice sheets is modeled in detail, and the particle physics of the interaction, including neutral and charged-current effects, fully-mixed neutrino flavors, and secondary shower production due to charged-current τ- and $\mu-$leptons are accounted for in the models. Finally, the detectors are also modeled with high fidelity, including the effects of Rician noise in the detection process, spectral response functions of the antennas, and full 3-D polarization propagation for the radio waves that interact with the detector. We thus have reason to report these performance estimates with confidence.

3.6.1 Sensitivity

The primary metric for detection of cosmogenic neutrinos, which are presumed to arrive isotropically on the sky, is the volumetric acceptance $\mathcal{V}\Omega$, in units of km^3 steradians. An equivalent parameterization is the areal acceptance $\mathcal{A}\Omega$ (km^2 sr) and the two are closely related by $\mathcal{A}\Omega = \mathcal{V}\Omega/\mathcal{L}_{int}(E_\nu)$ where $\mathcal{L}_{int}$ is the interaction length of the neutrinos as a function of neutrino energy E_ν. The volumetric acceptance, divided by the instrumented target fiducial volume, gives a measure of the detection efficiency of neutrinos which interact within the fiducial volume of a detector. In the case of ARA, one realization of the simulation uses a cylindrical ice target volume of radius 6 km, and depth 2 km. Because of earth attenuation, neutrinos arrive almost exclusively from above the horizon, giving a 2π factor for the solid angle. The net fiducial volumetric acceptance of this simulated ARA is thus just over 1400 km^3 sr, and this represents the maximum neutrino volumetric acceptance the simulation could obtain.

Figure 7 shows the $\mathcal{V}\Omega$ results for our adopted cluster baseline, as a function of neutrino energy in the range of interest for the cosmogenic flux. The acceptance reaches the level of ~ 100 km^3 sr at the mid-range of the cosmogenic neutrino flux, which has a broad plateau from about 5×10^{17} eV up to just over 10^{18} eV, and continues growing slowly up to the highest simulated energies. Note that, in our detected rate estimates, we have incorporated the most recent 2009 Auger results on cosmic ray composition and spectrum into our cosmogenic neutrino spectral modeling.

Figure 7 (bottom) gives a plot summary of some characteristics of the simulated data vs. neutrino energy. On the bottom left, the depth distribution of detected events is shown normalized to the event fraction per hundred meters. Events originating from below about 2 km depth are largely excluded, as the attenuation of the ice begins to grow quickly in the warmer basal ice. Figure 3 above shows both the attenuation lengths of the upper ~ 2 km of ice,
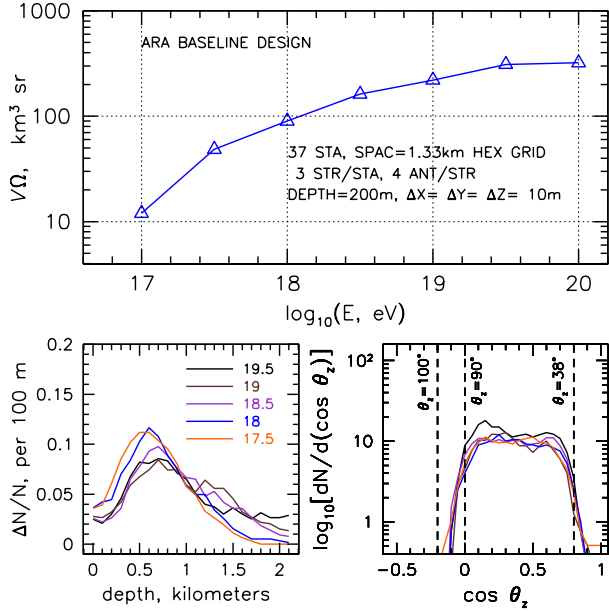
Figure 7: Top (large pane): Simulated neutrino volumetric acceptance (km^3 sr water equivalent) for the ARA instrument baseline design. Bottom left: Depth distribution of simulated events for different neutrino energies, showing the contribution of deep ice down to 2 km or more at the higher energies. Bottom right: zenith angle distribution of detected neutrino arrival directions for a range of neutrino energies. Events are detected over a range from $\sim 45°$ above the horizon to $\sim 5°$ below it.

which has an average temperature close to -50 C, and the complete ice column. The latter is dominated by the lossy deep ice, which reduces the overall average attenuation length to about 700-800 m. The attenuation length of our 2 km-deep fiducial volume is of order a factor of three better than ice in locations such as the Ross Ice Shelf, where the thickness is limited to several hundred meters, and the attenuation lengths are also comparable to this thickness scale. SP ice, especially in the upper 2km of its depth, is the clearest solid dielectric medium on Earth in the radio range, and is the most compelling natural feature of the ARA site.

Figure 7 (bottom) shows the arrival zenith angular distribution of detected neutrinos; the neutrino angular acceptance spans a range from $\sim 5°$ below the horizon to $\sim 45°$ above the horizon, more than 5 steradians of solid angle.

In Table 2 we give expected neutrino event totals for ARA for each year of operation, compared to recent published expectations for the best current limits to date, from the ANITA-1 flight [57]. It is evident that ARA in a single full year of operation improves on the ANITA-1 sensitivity by factors that vary between 10 and 40, and well over an order of magnitude on average over all of the models shown here. Over the planned instrument life of a decade or more, we expect to be able to not only establish

the flux levels for all of the most conservative models, but to be able to begin to measure their energy dependence as well. In the unlikely (and currently not self-consistent) case of an all-iron composition for the UHECR [62], ARA is also able within a few years to establish the presence or absence of even this highly suppressed GZK neutrino flux.

3.6.2 Resolution

Although not directly important for detection of neutrinos, the resolution of both the distance and angles to the neutrino interaction vertex, as well as the ability to reconstruct coarse neutrino incident directions on the sky, are important characteristics of our detector, and we have studied them in detail.

Our measurement of the distance to the neutrino vertex is accomplished by precise timing measurements of the wavefront curvature as it arrives at the cluster antenna array. This may be thought of as measuring the residuals when fitting the arrival times to a plane wave. For the angular measurements, the antenna array is analyzed as a correlation interferometer, and precise timing differences between the arrival times of the Askaryan radio impulse are determined for all of the $N(N-1)/2$ pairs of N antennas.

Complementing the precise timing measurements, we can also operate our cluster array as a radio intensity gradiometer and polarimeter. The gradiometric function comes through amplitude calibration of the received impulse, and the polarimetric information comes from ratios of the calibrated amplitudes of the Vpol and Hpol antennas.

All of these estimates are done in offline reconstruction routines. They are not necessary for the triggering of the array to record potential neutrino events, but they do make maximal use of the recorded information in the waveforms and arrival times of the events.

Vertex Resolution. The critical parameter for ver-

Table 2: Expected numbers of events N_ν from several UHE neutrino models, comparing published values from the 2006 ANITA-1 flight with predicted events per year from ARA.

| Model & references N_ν:	ANITA, 1st flt	ARA, yr^{-1}
Baseline BZ models		
Protheroe & Johnson 1996 [58]	0.22	7.0
Engel, Seckel, Stanev 2001 [59]	0.12	3.5
Barger, Huber, & Marfatia 2006 [60]	0.38	4.9
Strong source evolution BZ models		
Engel, Seckel, Stanev 2001 [59]	0.39	11.1
Barger, Huber, & Marfatia 2006 [60]	0.89	17.6
Yuksel & Kistler 2007 [61]	0.56	26.4
Waxman-Bahcall (WB) fluxes:		
WB 1999, evolved sources [17]	0.76	7.4
WB 1999, standard [17]	0.27	2.6
All-Iron UHECR composition:		
Ave et al. 2005 [62]	0.00	0.74
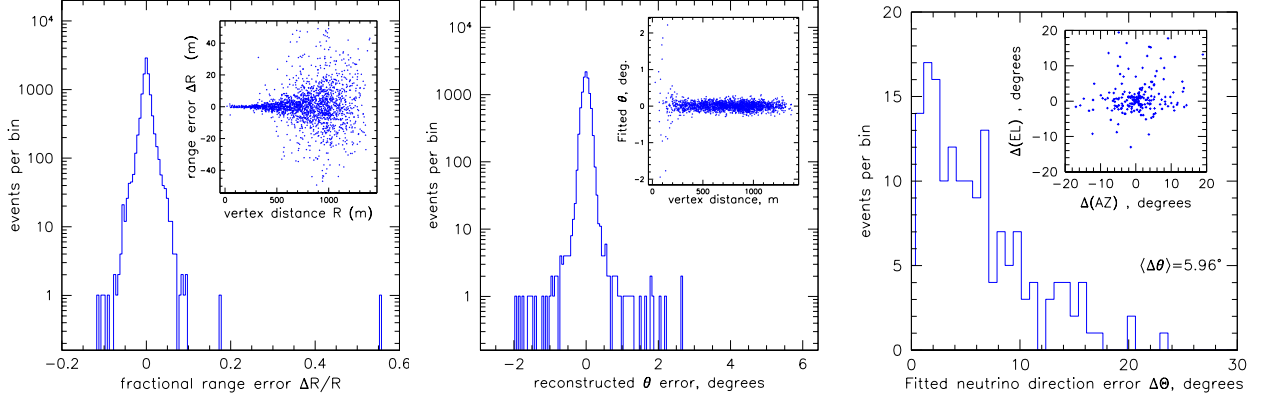
Figure 8: Left: Distribution of fractional range errors in single-antenna-cluster reconstruction of neutrino interaction vertex. Left inset: the distribution of reconstructed vertex range errors vs. range. Middle: Similar to left plot for reconstructed zenith angle of vertex relative to antenna cluster. Middle inset: distribution of reconstructed zenith angle vs. range to vertex. Right: Distribution of polar angle errors for full reconstruction of the incoming neutrino direction, using vertex reconstruction, amplitude, and polarization information. Right inset: the 2-D distribution of reconstructed directions relative to true neutrino direction.

tex location is the intra-cluster timing precision. For this we have used actual ANITA data, to which our collaboration has access. The ANITA payload, which uses waveform digitizers that are comparable to our planned digitizers, has demonstrated timing resolution as good as 30 ps rms for waveforms registered at the 4σ-level detection threshold of ANITA. This timing precision comes about from extensive in-flight calibration using ground-based impulse generators, and have proven robust in the ANITA analysis [63]. For our simulations we have derated these values by a factor of 3.3 to account for our more limited radio bandwidth, the slower sampling rate we expect to use, and for possibly unknown systematics in our calibration.

Figure 8 (left, middle) shows the results of these simulations for both the range and pointing resolution to the vertex. The latter values are important for determining whether an event originates under the ice or from above the ice, and the former values, combined with our knowledge of the ice attenuation, will bear directly on our ability to perform calorimetry on the neutrino shower.

Incident neutrino direction resolution. Estimating the neutrino vertex location in three dimensions does not immediately determine the arrival direction of the neutrino itself, and it may appear that the tight constraints of the cluster geometry would preclude determination of the neutrino direction, since this is normally done by imaging of the Cherenkov cone, at least in ring-imaging Cherenkov detectors. However, the richness of the radio wave information content does allow for first order Cherenkov cone determination, using both the amplitude gradient of the cone, and the polarization vector, which lies in the plane containing the Poynting vector of the

radiation and the shower momentum vector. Thus once the Poynting vector is determined via the vertex reconstruction, the plane of polarization combined with the local gradient in the cone amplitude is sufficient to constrain the neutrino direction on the sky.

To study the neutrino direction resolution, we have included first-order reconstruction algorithms in our Monte Carlo neutrino simulation. These do not yet perform a maximum likelihood minimization which would be very appropriate for this complex problem, but instead they perform a Ξ^2-grid search over variational parameters once the event has been detected in the simulation, which includes appropriate thermal noise backgrounds. These simulations are very compute-intensive, and involve full 3D ray-tracing of the radio propagation through the ice for each tested grid-point. Figure 8 (right) shows the results for about 80 detected events in a simulation run at $E_\nu = 3 \times 10^{18}$ eV. The reconstruction for these events was about 80% efficient (that is, 20% of the events failed to reconstruct), but the reconstructed zenith angle distribution shown has a very acceptable standard error of $\sim 6°$, the simplicity of our reconstruction code notwithstanding.

Energy Resolution. Once the event geometry has been reconstructed, the shower energy is determined via standard parametric equations [64, 44, 65]. The fractional error in shower energy due to a range error ΔR is $|\Delta E_{sh}/E_{sh}|_R = (1 + \alpha R)(\Delta R/R)$ where $\alpha = L_\alpha^{-1}$ is the ice attenuation coefficient and $\Delta R/R \sim 0.02$ from Figure 8. The variation with uncertainty in α is $|\Delta E_{sh}/E_{sh}|_\alpha = R(\Delta\alpha) \sim 0.3$ for events observed at one attenuation length and using Figure 3. We expect to reduce the uncertainty in α by direct measurement, thus reducing this contribu-

tion to $\Delta E_{sh}/E_{sh}$. The corresponding variation with neutrino direction is $|\Delta E_{sh}/E_{sh}|_\theta \simeq \Delta\theta\theta/\sigma^2$, where σ is the thickness of the radiation pattern around the Cerenkov cone, θ is the offset of the antenna with respect to the Cerenkov cone and $\Delta\theta$ is the error in neutrino direction. Since σ is a function of frequency, we anticipate improving the angular uncertainty of the neutrino direction, while improving the amplitude reconstruction. Finally an estimate of the neutrino energy from shower energy must account for the large variance in the Bjorken-y-distribution, defined by $E_\nu \simeq y^{-1}E_{sh}$ for charged-current ν_μ, ν_τ and all neutral-current events; electron neutrino events will be less affected by this, so our estimate is conservative. At neutrino energies of 10^{17-19} eV, numeric evaluations give $\langle y \rangle \simeq 0.22$, $\Delta y/y \simeq 1$, thus $|\Delta E_\nu/E_\nu|_y = \Delta y/\langle y \rangle \simeq 1$. Given our anticipated instrument capabilities we expect the energy resolution to be dominated by the Bjorken-y uncertainty. The y-dominated uncertainty is generic for UHE neutrino experiments, but this energy resolution is wholly adequate for the first-order science goals of the ARA instrument.

3.6.3 Comparison to Existing Instruments

Figure 9 provides a comprehensive graphic summary of the comparison of our estimated ARA sensitivity to estimates for several operating experiments, along with 2006 limits from the ARA forerunner experiment RICE [66]. We have already noted the comparison of ARA to the published ANITA limits; here we use projections for ANITA's reach after three flights, along with similar projections for IceCube and the Auger Observatory. GZK neutrino models are also included from a wide range of estimates [67, 68, 58, 59, 17, 62, 69], including the pure iron UHECR composition model noted above.

ARA improves over any other current instrument by an order of magnitude within 3 years of operation, filling in an important gap in sensitivity in the heart of the GZK neutrino spectral energy region. IceCube has excellent sensitivity to lower energies, up to the 10 PeV level, and ANITA has unmatched sensitivity at the higher energies, above 10 Eev. The Auger Observatory, while probing a similar energy range as ARA, does not have high neutrino sensitivity as it is primarily a UHECR instrument. ARA will complement these other instruments by making high sensitivity observations in the 0.1-10 EeV energy range, matching the peak of the expected GZK neutrino fluxes.
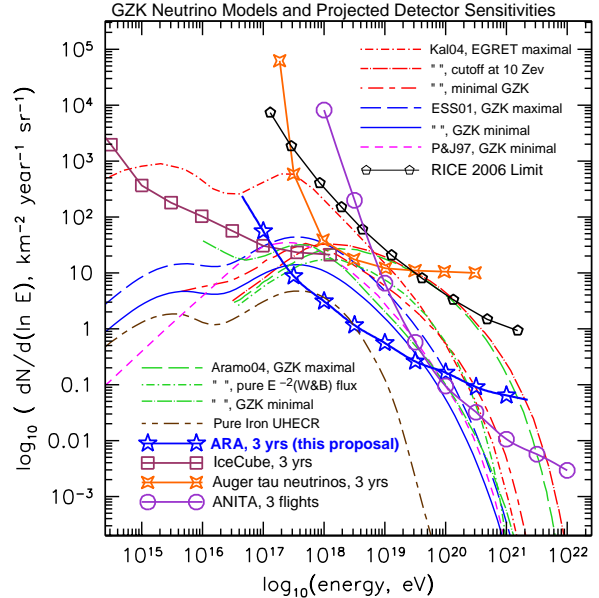

Figure 9: Compilation of sensitivity estimates from existing instruments, published limits, and a range of GZK neutrino models, along with the expected 3 year ARA sensitivity.

4 Broader Impact on Research and Training Infrastructure

In addition to drawing on the combined RICE + IceCube + ANITA scientific heritage that has resulted in ARA, this effort also takes advantage of three well-established and on-going education and outreach (E&O) programs. Rather than developing such activities over the course of the proposal, we will adapt and enlarge existing broader mission programs. The ARA physics goals are particularly well-matched to E&O: The mechanism behind the GZK suppression, where high energy protons interact with the CMB is so simple and elegant that it is readily accessible to a lay audience. Moreover, the adventurous nature of South Pole activity easily captures the imagination and ears of the general public (The recent Werner Herzog film ["*Encounters at the End of the World*"], which mentions ANITA prominently, attests to the public appeal of Antarctic science, and astrophysics, in particular.)

Student involvement, of course, figures prominently in the ARA broader mission. Both graduate and undergraduate level students will participate in simulation and detector calibration and construction at first, and in later stages in data analysis - thus exposing young scientists to neutrino astrophysics, RF technology and the on-site polar activities essential for a young scientist's development. Initial construction work also leads to the detailed familiarity with the hardware required by later studies of systematic errors. As noted in Table 1, undergraduate students are already making direct contributions –

in the category of simulations alone, undergraduates at the Universities of Maryland and Wisconsin are currently performing analysis of shower simulation outputs using Monte Carlo codes originally developed by undergraduates at the Universities of Kansas and Delaware, for example.

At the K-12 level, we are examining several activities (time capsules to be deployed with some of the ARA strings, e.g.) for middle-school aged kids to familiarize them with astronomy, neutrinos, and South Pole science. Several such hands-on activities are already well-underway; in addition to the IceCube-related programs cited below, at UH, KU, UMD, UW and UNL, existing cosmic ray detectors are in-use by local high schools, under the auspices of either QuarkNet or CROP (Cosmic Ray Observatory Project), based in Lincoln, NE. These detectors not only allow students to observe cosmic ray particles being registered in real-time, but also conduct elementary data analysis on objects arriving from either galactic or extragalactic sources. Plans to supplement the existing CROP scintillator planes with 50-200 MHz Yagi antennas, and thereby detect the radiofrequency signals that accompany air showers, will provide younger researchers a more direct entree' into radiowave cosmic ray detection. In addition to servicing the urban communities where large universities are typically located, these programs have been particularly successful in more rural locales, where the inter-school spacing is particularly well-suited to measurement of ultra-high energy cosmic rays.

Building on prior IceCube, RICE and ANITA E&O Efforts The IceCube E&O program predominantly operates by providing scientific content and personnel to several successful projects, among them Upward Bound, Polartrec, the Knowles Foundation's teachers program, the Exploratorium in San Francisco and QuarkNet. We will maintain, and strengthen our connection to all of these ongoing programs. Reciprocally, ARA will also contribute scientific content and personnel to support the existing IceCube E&O program whose activities address a number of broader issues facing the science and technology community, including: i) Providing quality K - 12 teacher professional development, and producing new inquiry-based learning materials that showcase ongoing research; ii) Increasing the diversity of the science and technology workforce by partnering with minority institutions and programs that serve underrepresented groups; and iii) Enhancing the general public's appreciation and understanding of science through informal learning opportunities, including broadcast media,

museums and website development. The existing IceCube website, e.g., is currently being updated to incorporate radio detection techniques. Web interfaces demonstrating RF wave processing and reconstruction techniques, with links to the publicly-available ARA data will further increase the exposure of graduate, undergraduate and high school students to neutrino detection.

It should be realized that the construction and engineering aspects of building large particle physics detectors have particular appeal to students of all ages and the public. Over the last five years, IceCube has been the dominant engineering activity at South Pole; ARA will take over this role as IceCube construction winds down.

Given its relatively low-budget, the RICE project relied heavily on talented undergraduates (and even local high school students selected through our involvement with QuarkNet). Of the 12 individuals that have traveled to the South Pole for RICE, fully half have been undergraduates, one of whom was a transfer student from Haskell Indian Nations University (Lawrence, KS). Currently, there are 12 undergraduates involved in RICE/NARC, as well as seven local high school students who have been funded via the QuarkNet Project. Most recently (June–August, 2009) three Lawrence high school students designed and built a slotted cylinder prototype, with adjustable height and slot dimensions. That prototype achieved excellent VSWR performance between 525 and 750 MHz (VSWR<3); we are currently working on extending this excellent frequency response to the lower frequencies more relevant for ARA.

By combining the science interest of cosmic rays with the traditional appeal of any NASA program, the ANITA project has received high marks for its E&O program. During its two launches (December 2006 and December 2008, respectively), interested persons were kept informed daily about the progress of the balloon through both the ANITA website (provided through NASA), as well as the up-to-date blog which tracked the progress of the balloon. An online blog will similarly appraise interested parties of the drilling and deployment progress of ARA, supplemented by periodic live webcasts from the South Pole, wherein any individual will be able to log in and interact with ARA personnel on-site. An ARA prototype station developed by ARA collaborators at UH will be commissioned on campus, so students and the public can gain first-hand experience with the hardware of the proposed observatory.

Since there are several women scientists on the

ARA team (K. Hoffman from UMD, D. Williams from UA, H. Landsman from UW and others), we find it especially important to encourage high school female students and young scientists to pursue degrees in science, via outreach activities for the general public, and in schools. Hoffman was recently the keynote speaker at a Montgomery County-wide high school teachers conference; an interview with Landsman was recently featured in an Israel-wide radio broadcast on neutrino detection. By continuing such efforts, as well as working with undergrad and grad students we hope to increase the visibility of women with advanced degrees in sciences.

Beyond Particle Astrophysics The opportunity to drill an array of 200-meter deep holes over such a large footprint offers benefits beyond particle astrophysics. Examples include the opportunities to perform precision mapping of glacial flow through the firn layer, as well as radioglaciological probes over a well-monitored area relative to the local englacial bulk flow. Such flow is expected to result in a preferred crystal orientation fabric (COF), with associated birefringent asymmetries. Provided snow samples can be taken from each hole as a function of depth, this array also offers an unparalleled opportunity to quantify impurity concentrations, both horizontally and also as a function of depth into the ice sheet. The potential for raising public interest in this experiment correspondingly far exceeds the immediate neutrino detection goal.

5 Management Plan

This proposal is based on a collaborative effort of University of Wisconsin-Madison and the University of Maryland as MRI institutions and several other national and international collaborators, some of whom have committed to providing contributions to the cost share. The summed cumulative budget for the linked proposals # 6936176 from UW Madison and # 6938564 from UMD College Park is $7,931,117 over 5 years, of which $5,496,409 (69.3%) is requested from the NSF and $2,434,708 (30.7%) will be contributed by collaborating institutions in the form of cash, equipment and in-kind labor.

The ARA collaboration consists of scientists and engineers of 10 national and 6 international Universities and laboratories. All institutions bring prior expertise in instrument design and data analysis to this project which is based on traditions of three projects: RICE [55], ANITA [70], and IceCube and related R&D efforts on detection of cosmogenic neutrinos at the South Pole [37, 38].

In order to allow effective task coordination all tasks are organized in the work break down structure (WBS) which is also used to organize the project budget. Wherever possible, institutions take responsibility for deliverables in the WBS to minimize dependencies and shipping of components. The WBS reflects this structure and details of the structure and the task responsibilities are documented in the budget justification. Primary institutional responsibilities for the project are as follows:

- Univ. of Wisconsin (Karle, Landsman, Haugen): Management, Drilling and deployment, cluster integration and testing, commissioning.
- Univ. of Maryland (Hoffman): Calibration, transmitters, supercluster hardware and integration, offline data processing, simulations.
- Univ. of Hawaii (Gorham, Varner): RF electronics and cluster design
- Kansas Univ. (Besson): Remote stations (power and communications infrastructure)
- UL Brussels (Hanson): Online (DAQ, global trigger, data reduction) and transient detection
- National Taiwan Univ. (Chen): Instrumentation subsystems

All other collaborating institutions listed in Table 1 have expressed interest and are expected to provide some support primarily in the area of simulation and data analysis. These efforts are not explicitly part of this project's budget. All of the foreign institutions are planning funding requests at their national funding agencies.

The organizational structure of the ARA project is shown in Figure 5. The PI and Co-PI's are responsible for task execution and for reporting to the funding agency. The collaboration is consulted with all matters that may impact the science objective and any other strategic questions. The higher level project organization follows the WBS. The resource coordinator tracks project-wide resource allocation and cost. The coordinators in the four main WBS categories bring excellent expertise and leadership experience from prior projects (IceCube, ANITA, RICE). However, while coordinators track progress in the project it is the institutional leads who are responsible to assure that tasks assigned to an institution are performed on budget and schedule.

5.1 Schedule

A detailed conceptual design has been presented in the instrument description. The final engineering design including subsystem tests will be completed in the first 2 years of the project schedule. An overview of high level schedule milestones for construction and deployment is shown in Table 3. Design reviews will be important milestones and
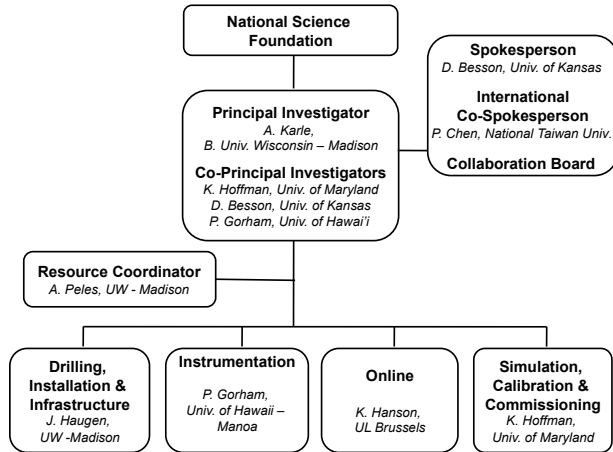
Figure 10: The proposed organization and management structure of the Askaryan Radio Array.

we will include experts from outside the collaboration on advisory and review panels when appropriate to ensure a critical assessment of design, production and construction plans. The construction schedule foresees the deployment of 4, 12, 12, 9 clusters during the construction seasons from 2011/12 to 2014/15.

5.2 Risks

We identify 3 risk elements and discuss measures for mitigation.

Table 3: Milestones for the array construction.

ID	Milestone	Owner	Date
1	Preliminary System Design Review. Include all major subsystem assemblies.	UMD	Sep 2010
2	Ship Testbed prototype instrumentation to Pole	UH	Oct 2010
3	Design, construct and ship to Pole the Ice Drill	UW	Aug 2011
4	Design, integrate, test and ship 4 pre-production In Ice Instrumentation clusters after Shipment Readiness Review.	UH	Sep 2011
5	Design, construct and test Remote Stations. Ship prototype to Pole after Shipment Readiness Review.	KU	Sep 2011
6	Commission Ice Drill	UW	Dec 2011
7	Install and Commission 4 Radio Stations at Pole	UW	Feb 2012
8	Final Critical Design Review & Production Readiness Review	KU	Apr 2012
9	Instrumentation Shipment Readiness Review. Initial verification of data stream showing detector will meet Science objectives.	UW	Sep 2012
10	Instrumentation Shipment Readiness Review. Final verification of data stream showing detector will meet Science objectives.	UMD	Sep 2013
11	Integrated, test and ship 33 production In Ice Instrumentation clusters.	UW	Sep 2014

EMI. Although RICE/NARC has already demonstrated powerful background reduction with hardware somewhat less sophisticated than that proposed herein, the possibility of new transmitter systems at the South Pole station could pose a risk. We will work closely with NSF as well with entities like the SPUC EMI sub-committee to avoid any conflicts and, if necessary, we will employ mitigation measures such as the directional and/or high-threshold veto techniques detailed previously.

Drilling. The current engineering analysis suggests that the RAM drill will work with the modifications planned. In order to minimize risks we plan to assemble a panel of drilling experts from IceCube, the Ice Drilling Design and Operation (IDDO) and others to provide critical feedback of our plans. We will give this item high attention since it is clearly a critical path item for the construction schedule. Overall, we are confident that drilling to the required depth is doable within the scope and schedule of this project.

Power. Although wind power has been explored and used in the Antarctic for several years, the concept to generate power by windmills contains risks of reliability as well as of EMI interference. We expect initial deployments to primarily rely on cable, but with redundant turbines. If, for any reason, the windmill concept does not pass all requirements on schedule, we will deploy cables until performance specifications are satisfied. Preliminary analysis shows that a backup strategy for the delivery of power and communications based on cables is realistic. Maintenance considerations will be included in risk assessments.

5.3 Maintenance and Operations (M&O) and data release

As documented in the ORW, the maintenance and operations of the experiment will start simultaneously with the construction phase. Aside from the yearly inspection of the wind turbines, the instrument itself will need very little maintenance, corresponding to an on-site presence of only a few people for several weeks. Support for M&O will be planned as a normal service work of scientists, postdocs and graduate students working on the experiment. This service work will allow also important training functions of students and postdocs.

The science collaboration plans to produce high level science data, which, once calibrated and reduced to physics events, will be released to the broader scientific community.

References

[1] P. Chen and K. D. Hoffman, Editors for interested physicists in the IceCube and ANITA Collaborations, Origin and evolution of cosmic accelerators - the unique discovery potential of an UHE neutrino telescope: Astronomy Decadal Survey (2010-2020) Science White Paper, (2009), arXiv:0902.3288.

[2] A. V. Olinto *et al.*, White Paper on Ultra-High Energy Cosmic Rays, (2009), arXiv:0903.0205.

[3] V. S. Berezinsky and G. T. Zatsepin, Cosmic neutrinos of superhigh energy, Yad. Fiz. **11**, 200 (1970).

[4] F. W. Stecker, Ultrahigh energy photons, electrons and neutrinos, the microwave background, and the universal cosmic ray hypothesis, Astrophys. Space Sci. **20**, 47 (1973).

[5] K. Greisen, End to the cosmic ray spectrum?, Phys. Rev. Lett. **16**, 748 (1966).

[6] G. T. Zatsepin and V. A. Kuzmin, Upper limit of the spectrum of cosmic rays, JETP Lett. **4**, 78 (1966).

[7] P. Blasi, Direct Measurements, Acceleration and Propagation of Cosmic Rays, (2008), arXiv:0801.4534.

[8] J. W. Cronin, The highest-energy cosmic rays, Nucl. Phys. Proc. Suppl. **138**, 465 (2005), arXiv:astro-ph/0402487.

[9] J. Linsley, Evidence for a primary cosmic-ray particle with energy 10^{20} eV, Phys. Rev. Lett. **10**, 146 (1963).

[10] HiRes, R. Abbasi *et al.*, Observation of the GZK cutoff by the HiRes experiment, Phys. Rev. Lett. **100**, 101101 (2008), arXiv:astro-ph/0703099.

[11] AGASA, M. Takeda *et al.*, Extension of the cosmic-ray energy spectrum beyond the predicted Greisen-Zatsepin-Kuzmin cutoff, Phys. Rev. Lett. **81**, 1163 (1998), arXiv:astro-ph/9807193.

[12] AUGER, J. Abraham *et al.*, The Cosmic Ray Energy Spectrum and Related Measurements with the Pierre Auger Observatory, (2009), arXiv:0906.2189.

[13] AUGER, J. Abraham *et al.*, Correlation of the highest-energy cosmic rays with the positions of nearby active galactic nuclei, Astropart. Phys. **29**, 188 (2008), arXiv:0712.2843.

[14] AUGER, J. Abraham *et al.*, Astrophysical Sources of Cosmic Rays and Related Measurements with the Pierre Auger Observatory, (2009), arXiv:0906.2347.

[15] D. Seckel and T. Stanev, Neutrinos: The key to UHE cosmic rays, Phys. Rev. Lett. **95**, 141101 (2005), arXiv:astro-ph/0502244.

[16] V. Berezinsky, A. Z. Gazizov, and S. I. Grigorieva, Dip in UHECR spectrum as signature of proton interaction with CMB, Phys. Lett. **B612**, 147 (2005), arXiv:astro-ph/0502550.

[17] E. Waxman and J. N. Bahcall, High energy neutrinos from astrophysical sources: An upper bound, Phys. Rev. **D59**, 023002 (1999), arXiv:hep-ph/9807282.

[18] K. Mannheim, R. J. Protheroe, and J. P. Rachen, On the cosmic ray bound for models of extragalactic neutrino production, Phys. Rev. **D63**, 023003 (2001), arXiv:astro-ph/9812398.

[19] E. Waxman and J. N. Bahcall, High energy neutrinos from cosmological gamma-ray burst fireballs, Phys. Rev. Lett. **78**, 2292 (1997), arXiv:astro-ph/9701231.

[20] P. Meszaros and S. Razzaque, Theoretical aspects of high energy neutrinos and GRB, (2006), arXiv:astro-ph/0605166.

[21] R. J. Protheroe and T. Stanev, Limits on models of the ultrahigh energy cosmic rays based on topological defects, Phys. Rev. Lett. **77**, 3708 (1996), arXiv:astro-ph/9605036.

[22] R. Gandhi, C. Quigg, M. H. Reno, and I. Sarcevic, Neutrino interactions at ultrahigh-energies, Phys. Rev. **D58**, 093009 (1998), arXiv:hep-ph/9807264.

[23] L. A. Anchordoqui, J. L. Feng, H. Goldberg, and A. D. Shapere, Neutrino Bounds on Astrophysical Sources and New Physics, Phys. Rev. **D66**, 103002 (2002), arXiv:hep-ph/0207139.

[24] S. Hussain, D. Marfatia, D. W. McKay, and D. Seckel, Cross section dependence of event rates at neutrino telescopes, Phys. Rev. Lett. **97**, 161101 (2006), arXiv:hep-ph/0606246.

[25] Super-Kamiokande, Y. Fukuda *et al.*, Measurement of the solar neutrino energy spectrum using neutrino electron scattering, Phys. Rev. Lett. **82**, 2430 (1999), arXiv:hep-ex/9812011.

[26] SNO, Q. R. Ahmad *et al.*, Direct evidence for neutrino flavor transformation from neutral-current interactions in the Sudbury Neutrino Observatory, Phys. Rev. Lett. **89**, 011301 (2002), arXiv:nucl-ex/0204008.

[27] Super-Kamiokande, Y. Fukuda *et al.*, Evidence for oscillation of atmospheric neutrinos, Phys. Rev. Lett. **81**, 1562 (1998), arXiv:hep-ex/9807003.

[28] IceCube, J. Ahrens *et al.*, Sensitivity of the IceCube detector to astrophysical sources of high energy muon neutrinos, Astropart. Phys. **20**, 507 (2004), arXiv:astro-ph/0305196.

[29] IceCube, A. Achterberg *et al.*, First year performance of the IceCube neutrino telescope, Astropart. Phys. **26**, 155 (2006), arXiv:astro-ph/0604450.

[30] ANTARES, O. Kalekin, The ANTARES underwater neutrino telescope, J. Phys. Conf. Ser. **160**, 012036 (2009).

[31] IceCube, R. Abbasi *et al.*, First Neutrino Point-Source Results From the 22-String IceCube Detector, Astrophys. J. **701**, L47 (2009), arXiv:0905.2253.

[32] IceCube, R. Abbasi *et al.*, Limits on a muon flux from neutralino annihilations in the Sun with the IceCube 22-string detector, Phys. Rev. Lett. **102**, 201302 (2009), arXiv:0902.2460.

[33] IceCube, R. Abbasi *et al.*, Search for high-energy muon neutrinos from the 'naked-eye' GRB 080319B with the IceCube neutrino telescope, Astrophys. J. **701**, 1721 (2009), arXiv:0902.0131.

[34] D. P. Hogan, D. Z. Besson, J. P. Ralston, I. Kravchenko, and D. Seckel, Relativistic Magnetic Monopole Flux Constraints from RICE, Phys. Rev. **D78**, 075031 (2008), arXiv:0806.2129.

[35] D. Besson, R. Keast, and R. Velasco, In situ and laboratory studies of radiofrequency propagation through ice and implications for siting a large-scale Antarctic neutrino detector, Astropart. Phys. **31**, 348 (2009).

[36] D. Besson, contributed to TeV09, manuscript in preparation .

[37] K. D. Hoffman, AURA: The Askaryan Underice Radio Array, J. Phys. Conf. Ser. **81**, 012022 (2007).

[38] H. Landsman *et al.*, AURA - A radio frequency extension to IceCube, (2008), arXiv:0811.2520.

[39] G. S. Varner, L. L. Ruckman, P. W. Gorham, J. W. Nam, R. J. Nichol, J. Cao, and M. Wilcox, The large analog bandwidth recorder and digitizer with ordered readout (LABRADOR) ASIC, Nucl. Instrum. Meth. **A583**, 447 (2007), arXiv:physics/0509023.

[40] G. A. Askaryan, Excess Negative Charge of an Electron-Photon Shower And Its Coherent Radio Emission, JETP Lett. **14**, 441 (1962).

[41] D. Saltzberg *et al.*, Observation of the Askaryan effect: Coherent microwave Cherenkov emission from charge asymmetry in high energy particle cascades, Phys. Rev. Lett. **86**, 2802 (2001), arXiv:hep-ex/0011001.

[42] P. W. Gorham *et al.*, Accelerator measurements of the Askaryan effect in rock salt: A roadmap toward Teraton underground neutrino detectors, Phys. Rev. **D72**, 023002 (2005), arXiv:astro-ph/0412128.

[43] ANITA, P. W. Gorham *et al.*, Observations of the Askaryan effect in ice, Phys. Rev. Lett. **99**, 171101 (2007), arXiv:hep-ex/0611008.

[44] J. Alvarez-Muniz, R. A. Vazquez, and E. Zas, Calculation methods for radio pulses from high energy showers, Phys. Rev. **D62**, 063001 (2000), arXiv:astro-ph/0003315.

[45] S. Boeser *et al.*, Feasibility of acoustic neutrino detection in ice: Design and performance of the South Pole Acoustic Test Setup (SPATS), (2008), arXiv:0807.4676.

[46] J. Vandenbroucke, for the IceCube Collaboration, Measurement of acoustic properties of South Pole ice for neutrino astronomy, (2008), arXiv:0811.1087.

[47] S. Barwick, D. Besson, P. Gorham, and D. Saltzberg, South Polar in situ radio-frequency ice attenuation, J. Glaciol. **51**, 231 (2005).

[48] P. B. Price, O. V. Nagornov, R. Bay, D. Chirkin, Y. He, P. Miocinovic, A. Richards, K. Woschnagg, B. Koci, and V. Zagorodnov, Temperature profile for glacial ice at the South Pole: Implications for life in a nearby subglacial lake, Proceedings of the National Academy of Sciences of the United States of America **99**, 7844 (2002), http://www.pnas.org/content/99/12/7844.full.pdf+html.

[49] G. Varner, The Modern FPGA as Discriminator, TDC and ADC, J. Instr. **1**, 07001 (2008).

[50] ANITA, G. Varner *et al.*, Detection of ultra high energy neutrinos via coherent radio emission, Proceedings of International Symposium on Detector Development for Particle, Astroparticle and Synchrotron Radiation Experiments (SNIC 2006), Menlo Park, California, 3-6 Apr 2006, pp 0046. SLAC-PUB-11872, SNIC-2006-0046

[51] http://facility.unavco.org/project_support/polar/remote/remote.html.

[52] http://space.augsburg.edu/ago/status.html.

[53] http://www.nsf.gov/awardsearch/showAward.do?AwardNumber=0531910.

[54] D. Seckel *et al.*, In-Ice radio detection of air shower cores, in Proceedings of 30th ICRC, Merida, Mexico, (2007).

[55] RICE, I. Kravchenko *et al.*, Performance and simulation of the RICE detector, Astropart. Phys. **19**, 15 (2003), arXiv:astro-ph/0112372.

[56] P. W. Gorham, C. L. Hebert, K. M. Liewer, C. J. Naudet, D. Saltzberg, and D. Williams, Experimental limit on the cosmic diffuse ultrahigh energy neutrino flux, Phys. Rev. Lett. **93**, 041101 (2004), arXiv:astro-ph/0310232.

[57] ANITA, P. Gorham *et al.*, New Limits on the Ultra-high Energy Cosmic Neutrino Flux from the ANITA Experiment, Phys. Rev. Lett. **103**, 051103 (2009), arXiv:0812.2715.

[58] R. J. Protheroe and P. A. Johnson, Propagation of ultrahigh-energy protons over cosmological distances and implications for topological defect models, Astropart. Phys. **4**, 253 (1996), arXiv:astro-ph/9506119.

[59] R. Engel, D. Seckel, and T. Stanev, Neutrinos from propagation of ultra-high energy protons, Phys. Rev. **D64**, 093010 (2001), arXiv:astro-ph/0101216.

[60] V. Barger, P. Huber, and D. Marfatia, Ultra high energy neutrino nucleon cross section from cosmic ray experiments and neutrino telescopes, Phys. Lett. **B642**, 333 (2006), arXiv:hep-ph/0606311.

[61] H. Yuksel and M. D. Kistler, Enhanced Cosmological GRB Rates and Implications for Cosmogenic Neutrinos, Phys. Rev. **D75**, 083004 (2007), arXiv:astro-ph/0610481.

[62] M. Ave, N. Busca, A. V. Olinto, A. A. Watson, and T. Yamamoto, Cosmogenic neutrinos from ultra-high energy nuclei, Astropart. Phys. **23**, 19 (2005), arXiv:astro-ph/0409316.

[63] ANITA, P. Gorham *et al.*, The Antarctic Impulsive Transient Antenna Ultra-high Energy Neutrino Detector Design, Performance, and Sensitivity for 2006-2007 Balloon Flight, (2008), arXiv:0812.1920.

[64] E. Zas, F. Halzen, and T. Stanev, Electromagnetic pulses from high-energy showers: Implications for neutrino detection, Phys. Rev. **D45**, 362 (1992).

[65] N. Lehtinen, P. Gorham, A. Jacobson, and R. Roussel-Dupre, FORTE satellite constraints on ultra-high energy cosmic particle fluxes, Phys. Rev. **D69**, 013008 (2004), arXiv:astro-ph/0309656.

[66] RICE, I. Kravchenko *et al.*, RICE limits on the diffuse ultra-high energy neutrino flux, Phys. Rev. **D73**, 082002 (2006), arXiv:astro-ph/0601148.

[67] O. E. Kalashev, V. A. Kuzmin, D. V. Semikoz, and G. Sigl, Ultra-high energy neutrino fluxes and their constraints, Phys. Rev. **D66**, 063004 (2002), arXiv:hep-ph/0205050.

[68] O. E. Kalashev, V. A. Kuzmin, D. V. Semikoz, and G. Sigl, Ultra-high energy cosmic rays from neutrino emitting acceleration sources?, Phys. Rev. **D65**, 103003 (2002), arXiv:hep-ph/0112351.

[69] AUGER, C. Aramo *et al.*, Earth-skimming UHE tau neutrinos at the fluorescence detector of Pierre Auger Observatory, Astropart. Phys. **23**, 65 (2005), arXiv:astro-ph/0407638.

[70] ANITA, P. W. Gorham, The ANITA cosmogenic neutrino experiment, Int. J. Mod. Phys. **A21S1**, 158 (2006).